Interdomain Interactions Underlying Activation of Cyclic Nucleotide–Gated Channels

Michael D. Varnum and William N. Zagotta*

Cyclic nucleotide–gated (CNG) ion channels are multimeric proteins that activate in response to the binding of cyclic nucleotide to intracellular domains. Here, an intramolecular protein–protein interaction between the amino-terminal domain and the carboxyl-terminal ligand-binding domain of the rat olfactory CNG channel was shown to exert an autoexcitatory effect on channel activation. Calcium-calmodulin, which modulates CNG channel activity during odorant adaptation, blocked this interaction. A specific deletion within the amino-terminal domain disrupted the interdomain interaction in vitro and altered the gating properties and calmodulin sensitivity of expressed channels. Thus, the amino-terminal domain may promote channel opening by directly interacting with the carboxyl-terminal gating machinery; calmodulin regulates channel activity by targeting this interaction.

Cyclic nucleotide–gated (CNG) ion channels of olfactory receptor cells and retinal photoreceptors play a fundamental role in the response to sensory stimuli by converting a chemical signal, a change in intracellular cyclic nucleotide concentration, into an electrical signal (*1*). Several channel domains have been identified as important for the conformational changes that occur during activation of these channels (*2*–*8*), but it is not known how these different domains interact during ligand-induced channel activation. In particular, the NH_2-terminal region plays a role in tuning the activation characteristics of olfactory and retinal CNG channels (*3*, *5*, *7*). The olfactory channel NH_2-terminal region confers a more favorable equilibrium for channel opening after ligand binding (*3*, *5*), and deletion of regions of the NH_2-terminal cytoplasmic domain of olfactory (*2*) or rod (*9*) channels creates functional channels with altered properties, which suggests that this part of the channel constitutes an autoregulatory domain. How does this region of the channel, distinct from the cyclic nucleotide–binding (CNB) domain and pore, exert such an influence on the gating of these channels? One possibility is that the NH_2-terminal domain might modify channel gating by specific interactions with other domains, thereby contributing to the stability of the activated channel.

To investigate the interdomain interactions involved in CNG channel activation, we performed protein–protein interaction assays between various CNG channel cytoplasmic domains expressed as fusion proteins in bacteria (*10*) (Fig. 1A). Recombinant CNG channel domains fused to glutathione *S*-transferase (GST) were purified with glutathione-Sepharose beads (immobilized) and used as an affinity matrix to test for interactions with other purified fusion proteins (input) lacking GST but containing an epitope tag (FLAG) at the COOH-terminus. The ability of one region of the CNG channel to specifically bind another region could then be directly observed by Western blotting. We used this assay to test the hypothesis that interactions between the NH_2 and COOH-terminal domains might account for the autoregulatory effect of the NH_2-terminal domain. The NH_2-terminal domain of the rat olfactory channel (Rolf N) specifically bound the COOH-terminal domains of either the rat olfactory (Rolf C) or the bovine rod (Brod C) channels (Fig. 1B). This interaction was robust and highly specific. An interaction between the bovine rod NH_2-terminal domain (Brod N) and either Brod C or Rolf C (Fig. 1B) or between Rolf N and the CNB domain of the catabolite gene activator protein (CRP) was not detected under these conditions (*11*) (Fig. 1B). The interaction between Rolf N and either Rolf C or Brod C may underlie the ability of the NH_2-terminal domain to influence channel opening and can explain the behavior of chimeric channels (*3*, *5*).

Another way that the NH_2-terminal domain might influence the gating properties of these channels is by mediating a change in intersubunit interactions among NH_2-terminal domains during channel opening (*3*, *7*). This idea was suggested by analogy to a family of proteins related to CNG channels, voltage-gated potassium

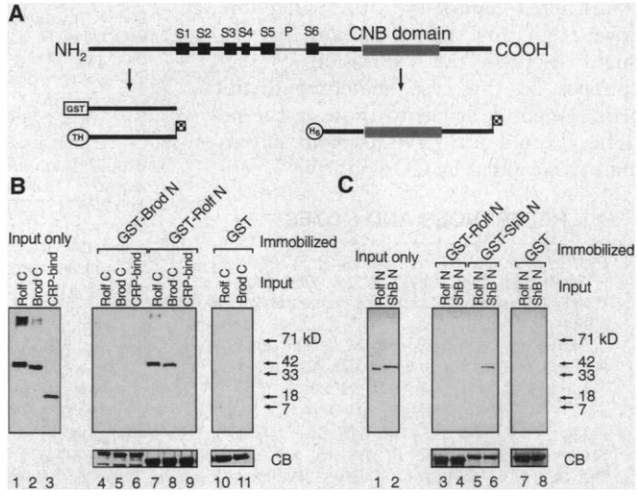

Fig. 1. Physical interaction in vitro of olfactory CNG channel NH_2-terminal domain with olfactory or rod channel COOH-terminal domains. (**A**) Diagram depicting primary structure of CNG channels and recombinant fusion proteins derived from NH_2- and COOH-terminal cytoplasmic domains. S1 to S6, putative membrane-spanning domains; P, pore region; TH, ThioHis fusion; H_6, polyhistidine tag; flag indicates epitope tag (FLAG). (**B**) Immunoblot of pairwise interaction assays with purified epitope-tagged input proteins and purified GST fusion proteins immobilized on glutathione-Sepharose beads. Lanes 1 to 3, immunoblot of input protein only. Recombinant input proteins included a six-histidine fusion at the NH_2-terminus and an eight–amino acid FLAG epitope tag at the COOH-terminus. Rolf C, amino acids 394 to 661 of the rat olfactory CNG channel subunit 1 (*28*); Brod C, amino acids 421 to 686 of the bovine rod CNG channel subunit 1 (*29*); CRP-bind, amino acids 4 to 138 of the catabolite gene activator protein (*11*). Interaction assays with these input proteins were done against immobilized GST-Brod N (lanes 4 to 6), GST-Rolf N (lanes 7 to 9), or GST alone (lanes 10 and 11). GST-Brod N includes amino acids 1 to 161 of the bovine rod CNG channel subunit 1 (*29*); GST-Rolf N includes amino acids 1 to 138 of the olfactory CNG channel subunit 1 (*28*). Boxes below show Coomassie-blue–stained gel (CB) of immobilized protein. (**C**) Immunoblot of pairwise NH_2-terminal–NH_2-terminal interaction assays. Lanes 1 and 2, blot of recombinant epitope-tagged input proteins alone (input only). Input Rolf N and ShB N were purified ThioHis fusion proteins (Invitrogen) that were FLAG-tagged at the COOH-terminus. ShB N construct included amino acids 1 to 5 and 47 to 227 of the voltage-gated potassium channel Shaker B (*30*). Interaction assays were carried out with immobilized fusion protein GST-Rolf N (lanes 3 and 4), GST-ShB N (lanes 5 and 6), or GST alone (lanes 7 and 8).

Department of Physiology and Biophysics, and Howard Hughes Medical Institute, Box 357370, University of Washington School of Medicine, Seattle, WA 98195, USA.

*To whom correspondence should be addressed. E-mail: zagotta@u.washington.edu

channels, which contain an NH_2-terminal oligomerization domain that directs subfamily-specific assembly of subunits (*12*). However, when this assay was used, we observed no interaction between Rolf N domains (Fig. 1C), even under the same conditions in which ShakerB potassium channel NH_2-terminal domains (ShB N) interacted (Fig. 1C). Thus, the hypothesis that intersubunit interactions among NH_2-terminal domains can explain the effect of the olfactory NH_2-terminal domain on channel gating is not supported. CNG channels may lack an NH_2-terminal oligomerization domain analogous to the one present in voltage-gated potassium channels. No amino acid homology between CNG channels and voltage-gated potassium channels is apparent in this region. An alternative possibility is that the affinity of Rolf N for homophilic assembly is much lower than that of ShB N (Fig. 1C) or of Rolf N for Rolf C (Fig. 1B). It is also possible that other regions near the NH_2-terminal intracellular domain, perhaps including the putative first transmembrane segment (*3*, *13*), are involved in oligomerization of CNG channel subunits.

To localize those regions of the COOH-terminal domain important for binding to the olfactory NH_2-terminal domain, we engineered various deletions of Brod C and Rolf C (Fig. 2A). These deletions were based on the known crystal structure of a homologous CNB protein, CRP (*14*) (Fig. 2B), and on previous structure–function studies of CNG channels. The linker region between the sixth putative transmembrane domain (S6) and the CNB domain is thought to participate in the opening conformational change after ligand binding; it contains sites for modulation of channel gating by Ni^{2+} (*4*, *5*), protons (*15*), and thiol-reactive agents (*16*, *17*). This region of the channel, also including the putative A α helix of the CNB domain, was found to be sufficient but not essential for interaction with Rolf N (Fig. 2, C and D). Amino acid residues within the putative C α helix of the CNB domain are important for ligand discrimination and are involved in stabilizing the opening allosteric conformational change (*3*, *6*, *18*). However, deletion of the putative B and C α helices did not disrupt the interaction of the COOH-terminal domain with the NH_2-terminal domain (Fig. 2C). Moreover, polypeptides including this region of the channel and extending to the COOH-terminus were not sufficient for binding to Rolf N (Fig. 2, C and D). The CNB domain alone was found to be sufficient to interact with the NH_2-terminal domain (Fig. 2D); indeed, the putative β-roll structure of the binding domain appeared adequate for binding to Rolf N (Fig. 2C). Overall, the interaction with Rolf N was probably mediated by the β-roll structure of the CNB domain and some portion of the putative A α helix and the linker between S6 and the CNB domain. Thus, the NH_2-terminal domain appears poised to exert a direct effect on ligand binding and on the subsequent conformational transitions leading to channel opening.

We applied a similar approach to determine which regions of the olfactory channel NH_2-terminal domain were important for interaction with the COOH-terminal domain. Various deletions were made in Rolf N (Fig. 3A), and these were tested for their ability to interact with Rolf C. Deletion of amino acids 3 to 60 or 93 to 138 of Rolf N did not prevent binding to Rolf C (Fig. 3B). However, a deletion encompassing amino acids 62 to 91 of Rolf N completely disrupted the interaction with Rolf C (Fig. 3B). This same region of the rat olfactory NH_2-terminal domain was previously identified as constituting part of the regulatory site for Ca^{2+}-calmodulin (*2*). Thus, these results identify a region of the NH_2-terminal domain that is essential both for binding of the COOH-terminal domain and for modulation by Ca^{2+}-calmodulin and suggest that the interdomain interaction may play a pivotal role in regulation of channel activity.

To examine the functional significance of this region of the NH_2-terminal domain in channel gating, Rolf CNG channels lacking amino acids 62 to 91 were expressed in *Xenopus* oocytes (*19*). As expected (*2*), these channels demonstrated dramatically altered gating properties. The apparent affinity for guanosine 3′,5′-monophosphate (cGMP) was about seven times less for Rolf Δ62–91 channels (13.8 ± 2.0 μM; $n = 5$) compared with wild-type (2.3 ± 0.4 μM; $n = 4$) or Δ3–60 (2.3 ± 0.2 μM; $n = 4$) channels (Fig. 3, C and D). Similarly, the apparent affinity for adenosine 3′,5′-monophosphate (cAMP) was also reduced for Rolf Δ62–91 channels (628 ± 375 μM; $n = 5$) compared with wild-type (74.4 ± 17.1 μM; $n = 4$) or Δ3–60 (76.1 ± 11.1 μM; $n = 4$) channels (Fig. 3E). Furthermore, the maximal current elicited by a saturating concentration of cAMP was decreased for Rolf Δ62–91 channels (Fig. 3, E and F). The effect of this deletion not only on the apparent affinity of the channel for cGMP and cAMP but also on the agonist efficacy of cAMP indicates that this region of the NH_2-terminal domain could participate in the opening allosteric conformational change after ligand binding. In addition,

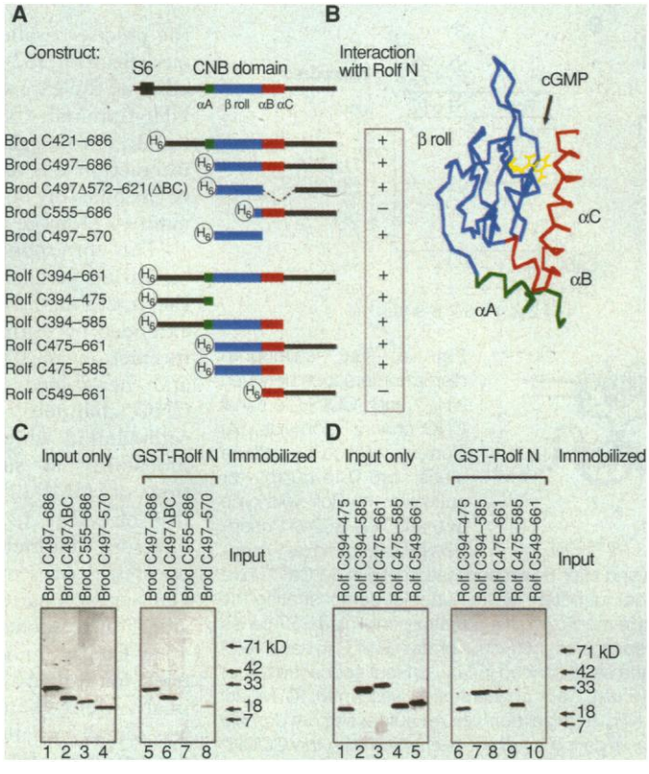

Fig. 2. Localization of regions in the CNG channel COOH-terminal intracellular domain important for interaction with the NH_2-terminal domain. (**A**) Deletion constructs for bovine rod or rat olfactory CNG channel COOH-terminal domains. Box on right summarizes results from interaction assays with GST-Rolf N shown in (C) and (D). H_6, polyhistidine fusion. CNB domain putative secondary structure: blue, β roll; green, A α helix; red, B and C α helices. (**B**) Model of CNB domain of the CNG channel based on analogy with the catabolite gene activator protein of *E. coli* (*14*). cGMP is shown in yellow. Putative structural motifs are indicated as in (A). (**C**) Immunoblot of interaction assays with the indicated Brod C deletions (input) and immobilized GST-Rolf N. Assays were done as described in Fig. 1. Blot of input only is shown on left. (**D**) Immunoblot of interaction assays using the indicated Rolf C deletions (input) and immobilized GST-Rolf N. Input only is shown on left.

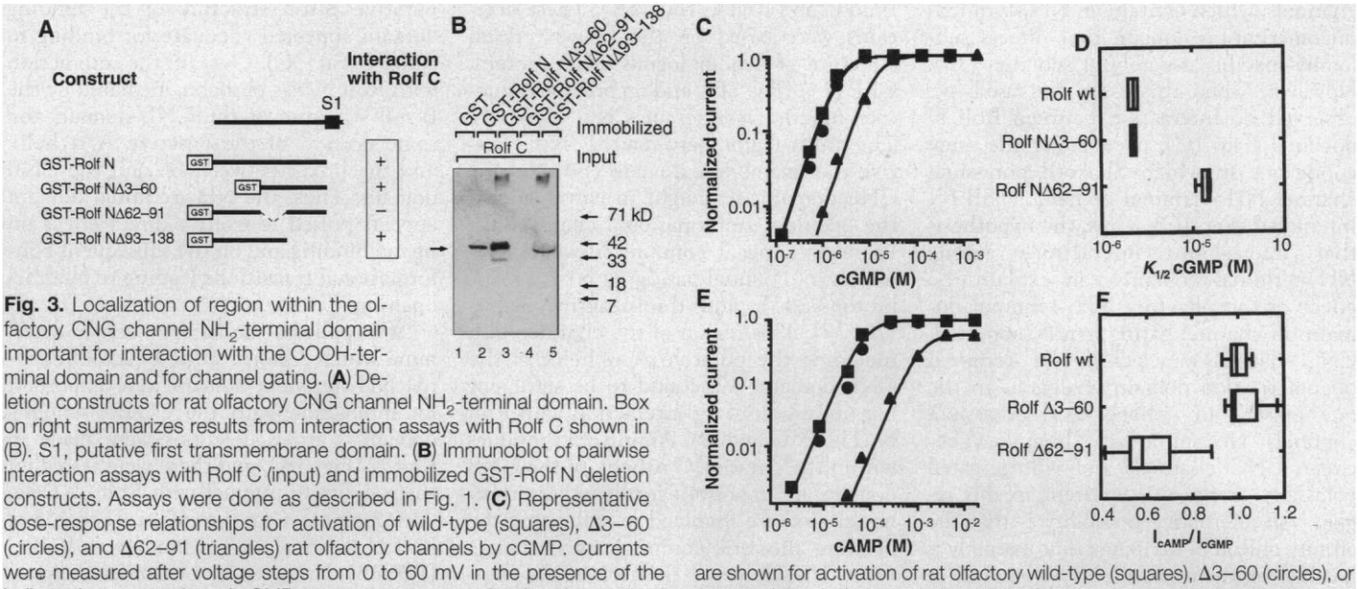

Fig. 3. Localization of region within the olfactory CNG channel NH_2-terminal domain important for interaction with the COOH-terminal domain and for channel gating. (**A**) Deletion constructs for rat olfactory CNG channel NH_2-terminal domain. Box on right summarizes results from interaction assays with Rolf C shown in (B). S1, putative first transmembrane domain. (**B**) Immunoblot of pairwise interaction assays with Rolf C (input) and immobilized GST-Rolf N deletion constructs. Assays were done as described in Fig. 1. (**C**) Representative dose-response relationships for activation of wild-type (squares), Δ3–60 (circles), and Δ62–91 (triangles) rat olfactory channels by cGMP. Currents were measured after voltage steps from 0 to 60 mV in the presence of the indicated concentration of cGMP; currents were normalized to the maximal current in saturating cGMP. Currents in the absence of cyclic nucleotide were subtracted. Continuous curves represent fits of the dose-response relationship to the Hill equation, $I/I_{max} = \{[cNMP]^n/(K_{1/2}{}^n + [cNMP]^n)\}$. For fits to the activation of Rolf wild-type and Δ3–60 channels by cGMP, the following parameters were used: $K_{1/2} = 1.95$ μM, $n = 1.9$, $I_{sat}/I_{max} = 1.0$. For fits to the activation of Rolf Δ62–91 channels by cGMP, the following parameters were used: $K_{1/2} = 13$ μM, $n = 1.9$, $I_{sat}/I_{max} = 1.0$. (**D**) Box plot of the apparent affinity ($K_{1/2}$) for cGMP of wild-type (wt) ($n = 4$), Δ3–60 ($n = 4$), and Δ62–91 ($n = 5$) rat olfactory channels from fits as shown in (C). Vertical line within each box indicates median of the data; boxes show 25th and 75th percentiles of the data; whiskers indicate range. (**E**) Representative dose-response relationships are shown for activation of rat olfactory wild-type (squares), Δ3–60 (circles), or Δ62–91 (triangles) channels by cAMP. Currents were normalized to maximal current elicited by saturating concentrations of cGMP. Continuous curves represent fits of the dose-response relationship to the Hill equation. For fits to the activation of Rolf wild-type and Δ3–60 channels by cAMP, the following parameters were used: $K_{1/2} = 70$ μM, $n = 1.8$, $I_{sat}/I_{max} = 1.0$. For fits to the activation of Rolf Δ62–91 channels by cAMP, the following parameters were used: $K_{1/2} = 1080$ μM, $n = 1.8$, $I_{sat}/I_{max} = 0.60$. (**F**) Box plot of ratio between the current elicited (at +60 mV) by a saturating cAMP concentration to that evoked by saturating cGMP, for Rolf wild-type (wt) ($n = 11$), Δ3–60 ($n = 9$), and Δ62–91 ($n = 7$) channels. This ratio is a measure of the agonist efficacy of cAMP and reflects the relative ability of these channels to undergo the allosteric transition associated with channel opening.

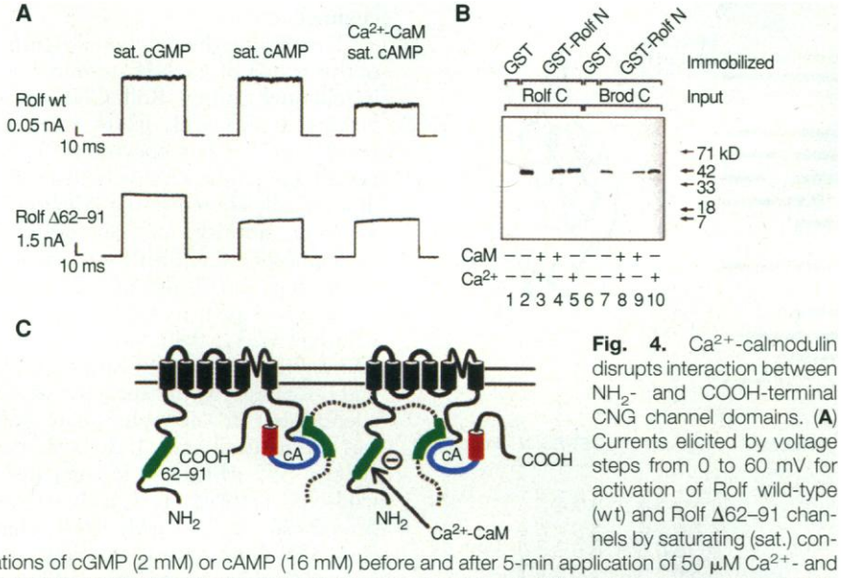

Fig. 4. Ca^{2+}-calmodulin disrupts interaction between NH_2- and COOH-terminal CNG channel domains. (**A**) Currents elicited by voltage steps from 0 to 60 mV for activation of Rolf wild-type (wt) and Rolf Δ62–91 channels by saturating (sat.) concentrations of cGMP (2 mM) or cAMP (16 mM) before and after 5-min application of 50 μM Ca^{2+}- and 250-nM calmodulin to the cytoplasmic face of an inside-out patch. (**B**) Immunoblot demonstrating the effect of Ca^{2+}-calmodulin on interaction assays with an immobilized affinity matrix containing GST (lanes 1 and 6) or GST-Rolf N (lanes 2 to 5 and 7 to 10) and epitope-tagged input protein Rolf C (lanes 1 to 5) or Brod C (lanes 6 to 10). Interaction assays were done as described in Fig. 1. Final concentration of calmodulin used during in vitro interaction assay was 15 μM; Ca^{2+} concentration was 1 mM. (**C**) Model for regulation of olfactory CNG channel gating by the NH_2-terminal domain. An autoexcitatory domain (green) within the NH_2-terminal region promotes channel gating by direct interaction with the COOH-terminal gating machinery, including the putative β-roll structure of the CNB domain (blue) but not the putative C α helix (red). This may be an intersubunit (left) or intrasubunit (right) association. The interaction is disrupted by binding of Ca^{2+}-calmodulin (Ca^{2+}-CaM) to the autoexcitatory domain. cA denotes cAMP.

the precise parallel between the deleterious effect of Δ62–91 on the gating properties of the expressed channel and on the NH_2-terminal–COOH-terminal interaction in vitro suggests that this interdomain interaction was responsible for the ability of the olfactory channel NH_2-terminal domain to promote channel opening.

This correspondence between an effect on gating of expressed channels and on the interdomain interaction in vitro was extended by testing the sensitivity of the interaction to Ca^{2+}-calmodulin. Native and heterologously expressed olfactory CNG channels are regulated by Ca^{2+}-calmodulin, which decreases the open probability at subsaturating concentrations of cGMP or a saturating concentration of cAMP (*2*, *20*). For wild-type rat olfactory channels expressed in *Xenopus* oocytes, macroscopic currents at +60 mV elicited by a saturating concentration of cAMP were decreased 30.8 ± 18.8% ($n = 4$) by Ca^{2+}-calmodulin (Fig. 4A). In contrast, for Rolf Δ62–91 channels the maximal current elicited by saturating cAMP was already smaller than that evoked by saturating cGMP in the absence of Ca^{2+}-calmodulin, and subsequent application of Ca^{2+}-calmodulin had no effect (Fig. 4A). We next examined the effect of Ca^{2+}-

calmodulin on the in vitro interaction between olfactory channel NH_2- and COOH-terminal intracellular domains. Addition of calmodulin in the presence of Ca^{2+} entirely disrupted the interaction between Rolf N and Rolf C (Fig. 4B). This effect was not observed with addition of either calmodulin alone or Ca^{2+} alone, which suggests that only calmodulin that has been activated by binding of Ca^{2+} can regulate this interdomain interaction. Similar results were obtained for the interaction between Rolf N and Brod C (Fig. 4B). Thus, these data define a region of the NH_2-terminal domain important for interdomain interactions, channel gating, and modulation of channel activity by Ca^{2+}-calmodulin.

We propose that the rat olfactory CNG channel NH_2-terminal domain promotes channel activation by direct interaction with the COOH-terminal gating machinery (Fig. 4C). Given the favorable contribution of this region of the olfactory channel to the free energy change for channel opening (*3*, *5*), we expect that the nature of this interaction may also exhibit some state dependence: the NH_2-terminal domain interacting more strongly with the COOH-terminal domain in the open conformation compared with the closed conformation of the channel, thus stabilizing the open state of the channel. However, we have not observed a pronounced cyclic nucleotide dependence for the in vitro interaction between NH_2- and COOH-terminal domains in these studies (*21*).

The interaction between olfactory CNG channel NH_2- and COOH-terminal domains was specifically blocked by Ca^{2+}-calmodulin. Adaptation to odorants in native olfactory receptor cells can be accounted for by a Ca^{2+} feedback mechanism acting primarily via Ca^{2+}-calmodulin regulation of olfactory CNG channels (*22*). Our results suggest a molecular mechanism for modulation of olfactory CNG channels by Ca^{2+}-calmodulin: binding of activated calmodulin to an autoexcitatory domain within the CNG channel NH_2-terminal domain, disrupting interdomain coupling with the COOH-terminal CNB domain. Heteromultimeric rod photoreceptor CNG channels are also modulated by Ca^{2+}-calmodulin (*23*), and this regulation may involve a similar disturbance of interdomain interactions.

The association of NH_2- and COOH-terminal domains may occur within the same subunit or between channel subunits (Fig. 4C). The latter possibility would provide a structural basis for concerted interactions between subunits during channel activation (*18*). Such an intersubunit interaction could also contribute to the association of CNG channel subunits into tetramers (*24*) and may govern the quaternary arrangement of heteromultimers formed with divergent CNG channel subunits (*25*). In this regard, CNG channels may differ somewhat from the related voltage-gated potassium channel family for which NH_2-terminal–NH_2-terminal interactions are the dominant determinant for subunit assembly (*12*). Significantly, under oxidizing conditions, rod CNG channels form an interdomain disulfide bond between NH_2- and COOH-terminal regions (*17*) and voltage-gated potassium channels display intersubunit interactions between NH_2- and COOH-terminal cysteine residues (*26*). This type of quaternary interaction may be a general feature of this ion-channel superfamily.

REFERENCES AND NOTES

1. W. N. Zagotta and S. A. Siegelbaum, *Ann. Rev. Neurosci.* **19**, 235 (1996).
2. M. Liu, T.-Y. Chen, B. Ahamed, J. Li, K.-W. Yau, *Science* **266**, 1348 (1994).
3. E. H. Goulding, G. R. Tibbs, S. A. Siegelbaum, *Nature* **372**, 369 (1994).
4. S. E. Gordon and W. N. Zagotta, *Neuron* **14**, 177 (1995).
5. ———, *ibid.*, p. 857 (1995).
6. M. D. Varnum, K. D. Black, W. N. Zagotta, *ibid.* **15**, 619 (1995).
7. G. R. Tibbs, E. H. Goulding, S. A. Siegelbaum, *Nature* **386**, 612 (1997).
8. A. F. Fodor, S. E. Gordon, W. N. Zagotta, *J. Gen. Physiol.* **109**, 3 (1997).
9. S. E. Gordon and W. N. Zagotta, *Proc. Natl. Acad. Sci. U.S.A.* **92**, 10222 (1995).
10. CNG channel intracellular domains were subcloned in frame with GST (pGEX-2TK or pGEX3X; Pharmacia), polyhistidine (pQE 30; Qiagen), or thioredoxin-histidine (pThioHis; Invitrogen) at the NH_2-terminus. Recombinant His-tagged or ThioHis fusion proteins were also engineered to include an 8–amino acid FLAG epitope (DYKDDDDK) (Eastman Kodak) at the COOH terminus. These constructs were transformed into *Escherichia coli* BL-21 (GST fusions) or M15 (His_6 or ThioHis fusions) strains; protein expression was induced by 0.25 mM isopropyl-β-D-thiogalactopyranoside at 25 to 30°C for 3 to 5 hours. Cells were harvested and resuspended in buffer S [50 mM tris-HCl (pH 7.8), 150 mM NaCl, 25 mM imidazole, 1% NDSB-256 (Calbiochem), 0.5% CHAPS detergent, and 0.25% Tween-20] containing protease inhibitors. Bacteria were lysed with a French press. Soluble protein was isolated by centrifugation at 20,000*g* at 4°C for 20 min. Glutathione-Sepharose beads (Pharmacia) were used to purify GST fusion proteins; His-tagged or ThioHis fusion proteins were purified with Ni-NTA beads (Qiagen) and eluted with 100 mM EDTA in buffer S. The ability of different recombinant proteins to interact was assayed by mixing various pairwise combinations in 0.5 ml of buffer S at 4°C overnight with shaking. The final concentration of immobilized GST fusion protein was about 25 to 50 μM (5 to 10 μl of glutathione-Sepharose beads; Pharmacia); the concentration of input protein was about 0.5 to 1 μM. Similar amounts of input protein were used for each assay as indicated in the input only blot. Beads were centrifuged at 2000*g* for 2 min and washed five times with 0.5 ml of buffer S. After the final wash, beads were resuspended in SDS–polyacrylamide gel electrophoresis (PAGE) sample buffer containing 2-mercaptoethanol, and bound proteins were separated by using denaturing 10 to 20% PAGE (Bio-Rad). After transfer to nitrocellulose, interacting input protein was visualized by using M2 monoclonal antibody (Eastman Kodak) directed against the FLAG epitope and the ECL chemiluminescence detection system (Amersham). Interaction assays were repeated at least three times with reproducible results.
11. H. Aiba, S. Fujimoto, N. Ozaki, *Nucleic Acids Res.* **10**, 1345 (1982); P. Cossart and S. B. Gicquel, *ibid.*, p. 1363.
12. M. Li, Y. N. Jan, L. Y. Jan, *Science* **257**, 1225 (1992).
13. N. V. Shen, X. Chen, M. M. Boyer, P. J. Pfaffinger, *Neuron* **11**, 67 (1993).
14. I. T. Weber and T. A. Steitz, *J. Mol. Biol.* **198**, 311 (1987).
15. S. E. Gordon, J. C. Oakley, M. D. Varnum, W. N. Zagotta, *Biochemistry* **35**, 3994 (1996).
16. J. T. Finn, J. Li, K.-W. Yau, *Biophys. J.* **68**, A253 (1995); M. C. Broillet and S. Firestein, *Neuron* **16**, 377 (1996).
17. S. E. Gordon, M. D. Varnum, W. N. Zagotta, *Neuron* **19**, 431 (1997).
18. M. D. Varnum and W. N. Zagotta, *Biophys. J.* **70**, 2667 (1996).
19. Oocyte preparation and complementary RNA transcription and expression were carried out as described (*27*). Patch-clamp experiments were performed with an Axopatch 200A amplifier (Axon Instruments) in the inside-out configuration. Currents were low-pass filtered at 2 kHz (8-pole Bessel) and sampled at 10 kHz. Recordings were made at 20 to 22°C. Data were acquired and analyzed with a Macintosh computer and Pulse software (Instrutech). Initial pipette resistances were 0.5 to 1 MΩ. Intracellular and extracellular solutions contained 130 mM NaCl, 0.2 mM EDTA, and 3 mM Hepes (pH 7.2). The pipette solution also included 500 μM niflumic acid to reduce endogenous Ca^{2+}-activated chloride currents; niflumic acid had no effect on cyclic nucleotide-activated currents (data not shown). For experiments with Ca^{2+}-calmodulin, EDTA in the intracellular solution was substituted with 704 μM $CaCl_2$, 2 mM nitrilotriacetate (50 μM free Ca^{2+} concentration) (*2*). Intracellular solutions containing cyclic nucleotides were changed with an RSC-100 rapid solution changer (Molecular Kinetics). Currents in the absence of cyclic nucleotide were subtracted.
20. T. Y. Chen and K. W. Yau, *Nature* **368**, 545 (1994).
21. M. D. Varnum and W. N. Zagotta, data not shown.
22. T. Kurahashi and A. Menini, *Nature* **385**, 725 (1997).
23. Y. T. Hsu and R. S. Molday, *ibid.* **361**, 76 (1993); T. Y. Chen *et al.*, *Proc. Natl. Acad. Sci. U.S.A.* **91**, 11757 (1994); S. E. Gordon, J. Downing-Park, A. L. Zimmerman, *J. Physiol. London* **486**, 533 (1995); M. E. Grunwald, W.-P. Yu, J. Li, K.-W. Yau, *Biophys. J.* **72**, A335 (1997).
24. D. T. Liu, G. R. Tibbs, S. A. Siegelbaum, *Neuron* **16**, 983 (1996).
25. T. Y. Chen *et al.*, *Nature* **362**, 764 (1993); J. Bradley, J. Li, N. Davidson, H. A. Lester, K. Zinn, *Proc. Natl. Acad. Sci. U.S.A.* **91**, 8890 (1994); E. R. Liman and L. B. Buck, *Neuron* **13**, 611 (1994).
26. C. T. Schulteis, N. Nagaya, D. M. Papazian, *Biochemistry* **35**, 12133 (1996).
27. W. N. Zagotta, T. Hoshi, R. W. Aldrich, *Proc. Natl. Acad. Sci. U.S.A.* **86**, 7243 (1989).
28. R. S. Dhallan, K. W. Yau, K. A. Schrader, R. R. Reed, *Nature* **347**, 184 (1990).
29. U. B. Kaupp *et al.*, *Nature* **342**, 762 (1989).
30. D. M. Papazian, T. L. Schwarz, B. L. Tempel, Y. N. Jan, L. Y. Jan, *Science* **237**, 749 (1987).

31. We thank K. Black, H. Utsugi, and G. Sheridan for expert technical assistance. We also gratefully acknowledge J. Hurley, M. Shapiro, G. Eaholtz, A. Fodor, and L. Sunderman for comments on the manuscript, and C. Tancioco for stimulating input. Supported by a grant from the National Eye Institute (EY 10329 to W.N.Z.). W.N.Z. is an Investigator and M.D.V. is an Associate of the Howard Hughes Medical Institute.

20 June 1997; accepted 18 August 1997